Cell Host & Microbe
Article

# Virulence of *Mycobacterium tuberculosis* Depends on Lipoamide Dehydrogenase, a Member of Three Multienzyme Complexes

Aditya Venugopal,[1,2] Ruslana Bryk,[1] Shuangping Shi,[1,2] Kyu Rhee,[3] Poonam Rath,[1,2] Dirk Schnappinger,[1] Sabine Ehrt,[1,2] and Carl Nathan[1,2,*]
[1]Department of Microbiology and Immunology, Weill Cornell Medical College, 1300 York Avenue, New York, NY 10065, USA
[2]Program in Immunology and Microbial Pathogenesis, Weill Graduate School of Medical Sciences, Cornell University, 1300 York Avenue, New York, NY 10065, USA
[3]Division of Infectious Diseases, Department of Medicine, Weill Cornell Medical College, 1300 York Avenue, New York, NY 10065, USA
*Correspondence: cnathan@med.cornell.edu
DOI 10.1016/j.chom.2010.12.004

## SUMMARY

*Mycobacterium tuberculosis* (Mtb) adapts to persist in a nutritionally limited macrophage compartment. Lipoamide dehydrogenase (Lpd), the third enzyme (E3) in Mtb's pyruvate dehydrogenase complex (PDH), also serves as E1 of peroxynitrite reductase/peroxidase (PNR/P), which helps Mtb resist host-reactive nitrogen intermediates. In contrast to Mtb lacking dihydrolipoamide acyltransferase (DlaT), the E2 of PDH and PNR/P, Lpd-deficient Mtb is severely attenuated in wild-type and immunodeficient mice. This suggests that Lpd has a function that DlaT does not share. When DlaT is absent, Mtb upregulates an Lpd-dependent branched-chain keto acid dehydrogenase (BCKADH) encoded by *pdhA*, *pdhB*, *pdhC,* and *lpdC*. Without Lpd, Mtb cannot metabolize branched-chain amino acids and potentially toxic branched-chain intermediates accumulate. Mtb deficient in both DlaT and PdhC phenocopies Lpd-deficient Mtb. Thus, Mtb critically requires BCKADH along with PDH and PNR/P for pathogenesis. These findings position Lpd as a potential target for anti-infectives against Mtb.

## INTRODUCTION

Most cases of tuberculosis are curable by drugs that have been available for more than 40 years, yet Mtb is the single leading cause of death from bacterial infection (Bloom and Murray, 1992). This medical-societal failure stems in part from using anti-infectives that are chiefly active against replicating bacteria to treat an infection in which many of the bacteria are not replicating (McCune et al., 1966; Nathan, 2009; Nathan et al., 2008). During a multi-decade innovation gap in anti-infective drug development (Fischbach and Walsh, 2009), the inexorable progression of drug resistance has made tuberculosis increasingly harder to treat and sometimes untreatable (Chan et al., 2008; Glaziou et al., 2009). Thus, a basic biologic question has acquired urgent medical relevance: on what gene products does Mtb depend for survival in the host? This is distinct from how the question is usually framed in antibacterial drug development: on what gene products does the pathogen depend for survival in vitro?

Whether Mtb infection is latent or active, many of the bacilli reside in macrophage phagosomes (Russell, 2001), where they can sustain net rates of population growth near zero for long periods (Gill et al., 2009; Munoz-Elias et al., 2005). Knowledge is growing about the metabolic pathways required for survival and persistence of intraphagosomal Mtb (Barry et al., 2009; Smith, 2000). Mtb requires the enzymes isocitrate lyases 1 and 2 (encoded by *icl1* and *icl2* and serving the glyoxylate shunt and methylcitrate cycle) to establish infection in the mouse (Munoz-Elias and McKinney, 2005) and also needs genes required for cholesterol metabolism to persist (Pandey and Sassetti, 2008). Additionally, upregulation of gluconeogenic and glyoxylate shunt genes in Mtb recovered from mouse macrophages (Schnappinger et al., 2003), mouse lungs, and patient specimens (Timm et al., 2003) suggests that to survive in the host, Mtb must metabolize acetyl coenzyme A (coA) in an anaplerotic fashion. It has been assumed that this reflects the derivation of acetyl coA from β-oxidation of fatty acids (Munoz-Elias and McKinney, 2006).

Anabolism of the branched-chain amino acids leucine, isoleucine, and valine has been well studied in Mtb and pathways responsible for their synthesis are essential for virulence (Hondalus et al., 2000). However, little attention has been given to their catabolism, which might serve to prevent their overaccumulation, facilitate the generation of branched-chain fatty acids, or provide energy.

One aspect of host-immune chemistry that contributes substantially to Mtb's nonreplication in vivo is the generation of reactive nitrogen intermediates (RNI) by inducible nitric oxide synthase (iNOS) (MacMicking et al., 1997). RNI can kill bacteria by forming intrabacterial peroxynitrite (St John et al., 2001). Accordingly, we searched for enzymes that permit Mtb to survive exposure to RNI. We discovered a PNR/P consisting of four enzymes: Lpd, encoded by *lpdC* (Rv0462) (Argyrou and Blanchard, 2001); DlaT; a thioredoxin-like protein, AhpD; and the peroxiredoxin AhpC (Bryk et al., 2000, 2002). Enzymes that function in complexes are often designated "E1," "E2," etc. in

the order of sequential catalysis. Lpd was originally predicted to serve as the last enzyme (E3) in two complexes, α-ketoglutarate dehydrogenase (αKGDH) and PDH in Mtb (Cole and Barrell, 1998). However, we found that Mtb lacks αKGDH (Tian et al., 2005a) and that the E1 and E2 of PDH are products of *aceE* and *dlaT* (Tian et al., 2005b), the latter originally misannotated as E2 of αKGDH. This left unexplained the functions of the proteins encoded by the genes *pdhA* (Rv2497c, annotated as the α subunit of E1 of PDH), *pdhB* (Rv2496c, annotated as the β subunit of E1 of PDH) and *pdhC* (Rv2495c, annotated as E2 of PDH). In many organisms Lpd is also the E3 of BCKADH, so we hypothesized that the *pdhABC* operon may encode the E1 and E2 of BCKADH (Tian et al., 2005b). However, we could detect no such activity in Mtb (Tian et al., 2005b).

Deletion of *dlaT* had a pronounced effect on Mtb's growth in standard medium in vitro, sensitized Mtb to RNI, and attenuated Mtb in the mouse (Shi and Ehrt, 2006). Additionally, species-selective DlaT inhibitors selectively killed nonreplicating Mtb (Bryk et al., 2008). We then focused on Lpd as a potential target, because it participates in the same two enzyme complexes as DlaT, namely PDH and PNR/P (Bryk et al., 2000, 2002). Structural differences between the active sites of human and mycobacterial Lpd (Rajashankar et al., 2005) were exploited in the development of species-selective inhibitors of mycobacterial Lpd (Bryk et al., 2010). In the course of these studies we were surprised to discover that Lpd-deficient Mtb was far more attenuated in vivo than DlaT-deficient Mtb. This led us to search for yet another function of Lpd. The findings add to our understanding of host-pathogen interactions in experimental tuberculosis.

## RESULTS

### Mtb Requires Lpd for Virulence

We disrupted *lpdC* in Mtb H37Rv by homologous recombination and confirmed the deletion by Southern blot (see Figure S1A, available online), mRNA analysis (see Figure S1B) and western blot (Figure 1A). We reintroduced *lpdC* via complementation in an integrative vector driven by a constitutive *hsp60* promoter and achieved wild-type expression levels of Lpd mRNA (see Figure S1B) and protein (Figure 1A). As will be shown subsequently, the Lpd-deficient strain grew, albeit poorly, in standard medium with dextrose, glycerol, and fatty acids as carbon sources. To confirm Lpd's role in metabolism of carbohydrates through its participation in PDH, we monitored the growth of wild-type, mutant, and complemented bacteria with glycerol and dextrose as the only carbon sources. As predicted, the Lpd-deficient bacteria failed to grow on carbohydrates, while the wild-type and complemented strains grew normally (Figure 1B). The Lpd-containing PNR/P detoxifies peroxynitrite but not NO (Bryk et al., 2000, 2002). Killing of bacteria by mildly acidified nitrite or other NO donors requires oxygen and involves oxidation of intrabacterial peptidyl methionine (St John et al., 2001), strongly suggesting that it proceeds through intrabacterial conversion of NO (a nonoxidizing species) to peroxynitrite (a strong oxidant). Thus, to test Lpd's role in PNR/P, we exposed the three strains to mildly acidified nitrite. The Lpd-deficient bacteria lost three $\log_{10}$ colony-forming units (CFUs) at concentrations of nitrite that reduced the viability of the wild-type and complemented strains by only <0.5 $\log_{10}$ (Figure 1C), consistent with Lpd's

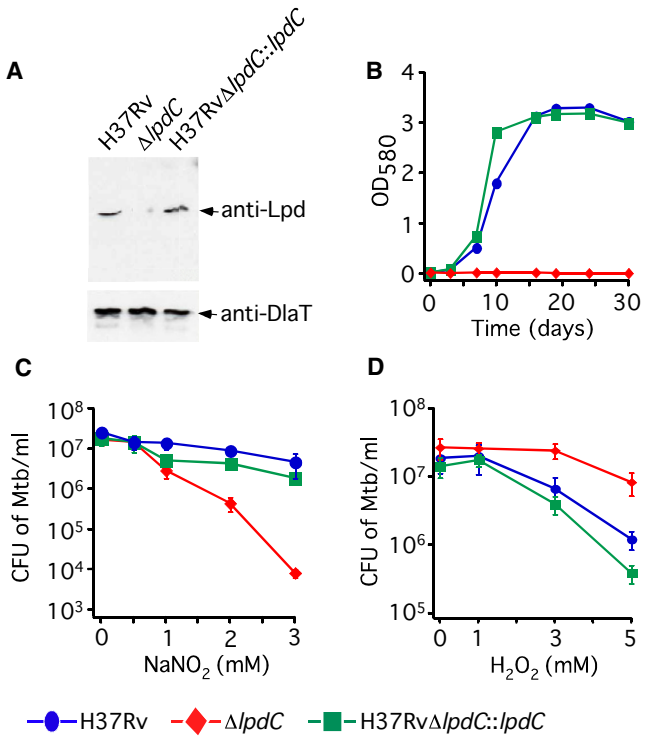


**Figure 1. Characterization of Lpd-Deficient Mtb In Vitro**

(A) Western blot analysis of wild-type (H37Rv), mutant (Δ*lpdC*), and complemented (H37RvΔ*lpdC*::*lpdC*) strains with antiserum against Lpd. Anti-DlaT was used to assess equal loading.

(B) Growth curve in bacteriologic medium containing dextrose and glycerol as the sole carbon sources.

(C) Survival of strains after 4 days exposure to $NaNO_2$ at pH 5.5. Means ± standard deviation (SD) of triplicate experimental samples are shown from one experiment, representative of three.

(D) Survival of strains upon exposure to increasing concentrations of $H_2O_2$ for 4 hr. Means ± SD of triplicate experimental samples are shown from one experiment, representative of two.

role in PNR/P. To determine whether Mtb lacking *lpdC* was specifically resistant to the stresses imposed, or merely sickly, we exposed wild-type, mutant, and complemented strains to oxidative stress in the form of $H_2O_2$. Mtb lacking *lpdC* was more resistant than wild-type and complemented strains, a property shared by several other Mtb mutants that are more sensitive to RNI in vitro (Darwin et al., 2003; Gandotra et al., 2007) (Figure 1D).

Next we assessed the role of Lpd in Mtb's ability to grow and persist in vivo by infecting C57BL/6 mice with Lpd-deficient Mtb or the wild-type or complemented strains. The mutant strain was rapidly cleared from the lungs (Figure 2A) and either never seeded the spleen or failed to survive there (Figure 2B). Because we plated the organs in their entirety, the detection limit in our assays was one CFU/organ. Nondetection of CFU did not result from toxicity of lung homogenates to the bacteria, because the expected number of CFU was observed by using the same homogenization procedure on the first day after infection. Lungs contained no detectable CFU in most of the mice from day 7 through termination of the experiment at day 164 and spleens contained no CFU at any time tested (days 28, 64, and 164).

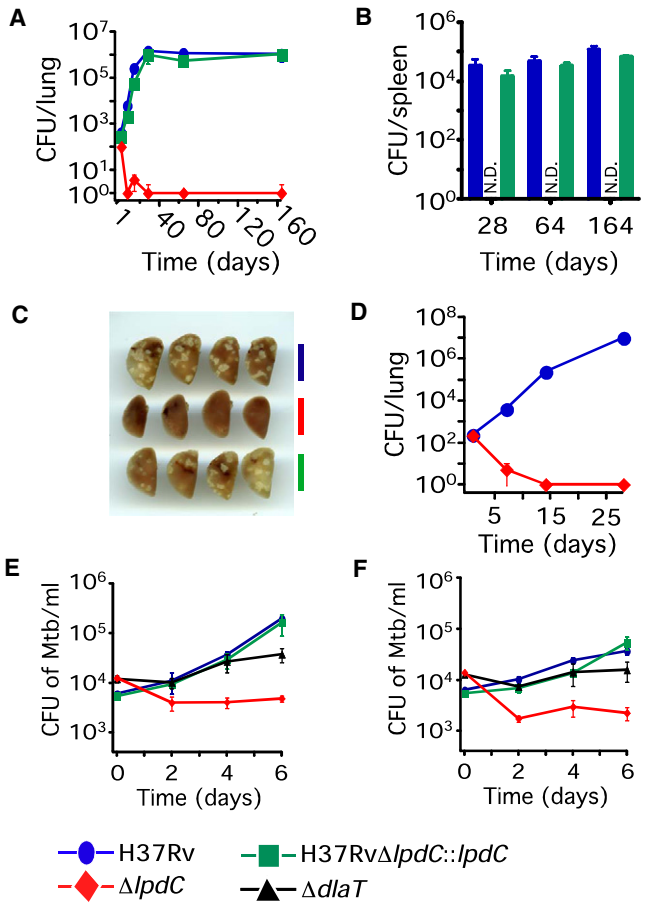


**Figure 2. Mtb Requires Lpd for Virulence in Both Wild-Type and IFNγ$^{-/-}$ Mice and in Macrophages**

(A, B) Fate of Mtb strains in C57BL/6 mice in (A) lungs and (B) spleens after aerosol infection. Means ± SD for four mice per point are shown from one experiment, representative of three.

(C) Gross pathology of lungs was recorded at day 164 postinfection.

(D) Survival of Mtb strains in mice lacking IFNγ. Means ± SD are shown from one experiment for four mice per point.

(E, F) Survival in naive (E) and IFNγ-activated (F) macrophages of the above Mtb strains, as well as in Mtb lacking *dlaT*. Means ± SD of triplicate experimental samples are shown from one experiment, representative of two.

Moreover, the lungs of mice infected with the *lpdC* mutant displayed no gross or microscopic pathology (Figure 2C and Figure S2). Complementation of the mutant restored virulence in vivo, confirming that the severe attenuation of the mutant in vivo was due to loss of *lpdC*.

Infection with Mtb elicits IFNγ production first by natural killer (NK) cells and then by T lymphocytes. IFNγ is critically required for control of Mtb infection in both mice and humans (Flynn et al., 1993; Jouanguy et al., 1997; Zhang et al., 2008). To test whether Mtb lacking *lpdC* requires IFNγ-dependent immunity for clearance of the bacterium, we infected IFNγ$^{-/-}$ mice. IFNγ$^{-/-}$ mice infected with the *lpdC* mutant rapidly cleared the infection, while those infected with wild-type Mtb were highly susceptible (Figure 2D).

Consistent with the rapid clearance of Lpd-deficient Mtb in vivo, bone marrow-derived macrophages from C56BL/6 mice killed the *lpdC* mutant by ~5 fold even without immunologic activation, while the wild-type and complemented strains grew ~1.5 $\log_{10}$ over the same period (Figure 2E). When macrophages were activated with IFNγ and then infected, the *lpdC* mutant was killed by ~1 $\log_{10}$ while the wild-type and complemented strains still grew, albeit more slowly than in naive macrophages (Figure 2F). The lesser effect of IFNγ in these experiments than in earlier studies (e.g., Shi and Ehrt, 2006) was associated with use of different IFNγ preparations and our current practice of omitting all antibiotics during the differentiation of the macrophages.

## Metabolic Differences between DlaT-Deficient and Lpd-Deficient Mtb

Characterization of DlaT-deficient Mtb in the same mouse model had revealed only a 1.5 $\log_{10}$ reduction in CFU in the lungs at the onset of the chronic stage of the infection compared to wild-type Mtb (Shi and Ehrt, 2006). The ≥6 $\log_{10}$ attenuation that we observed here with Lpd-deficient Mtb suggested that Lpd serves an important function in Mtb in which DlaT does not participate. Lpd-deficient and DlaT-deficient mutants were almost indistinguishable in their survival during exposure to a cell-wall-perturbing agent (SDS) (see Figure S3A) or lipophilic antibiotics (see Figures S3B–S3D). Both mutants, however, were more resistant to ethambutol and rifampicin than wild-type Mtb, possibly because of the impaired replication of these strains.

However, compared to DlaT-deficient Mtb, Lpd-deficient Mtb had an inferior capacity for extended growth in 7H9 medium (Figure 3A). Along with carbohydrates, 7H9 medium provides fatty acids when it is supplemented in the standard manner with the dispersal agent Tween 80 (an oleic acid polymer) and bovine serum albumin (a fatty acid carrier). The *lpdC* mutant did not merely cease growth at later time points, but died, as reflected by ~1 log loss of CFU, while wild-type, DlaT–deficient, and complemented Mtb continued to survive in stationary phase (Figure 3B). Removing dextrose and glycerol impaired the growth of wild-type Mtb as well as the *dlaT* mutant so that their growth rates became almost indistinguishable from that of the *lpdC* mutant (Figure 3C). This suggested that when carbohydrates were present, DlaT-deficient Mtb may have metabolized carbohydrates along with the fatty acids, while Lpd-deficient Mtb may have subsisted only on the fatty acids.

In order to elucidate a potential mechanism by which the *dlaT* mutant, despite lacking PDH, was able to use carbohydrates, we quantified several intracellular metabolites in wild-type and mutant bacteria. Inhibition of PDH by genetic deletion of either *lpdC* or *dlaT* is expected to lead to a buildup of glycolytic intermediates and pyruvate (Bryk et al., 2008). We grew the wild-type, mutant, and complemented strains on filter discs on 7H9 agar plates to facilitate rapid harvest and to avoid losing the metabolites that leak during handling (de Carvalho et al., 2010a, 2010b) and analyzed metabolites in their lysates by liquid chromatography-mass spectrometry. At week 2 of in vitro culture, by which time the *lpdC* and *dlaT* mutants had grown to a similar extent, pyruvate was comparably elevated in both mutant strains compared to wild-type and complemented strains (Figure 4A). Alanine, a metabolite of pyruvate, was also elevated in both mutant strains (see Figure S4A). The branched-chain amino acids valine, leucine, and isoleucine can

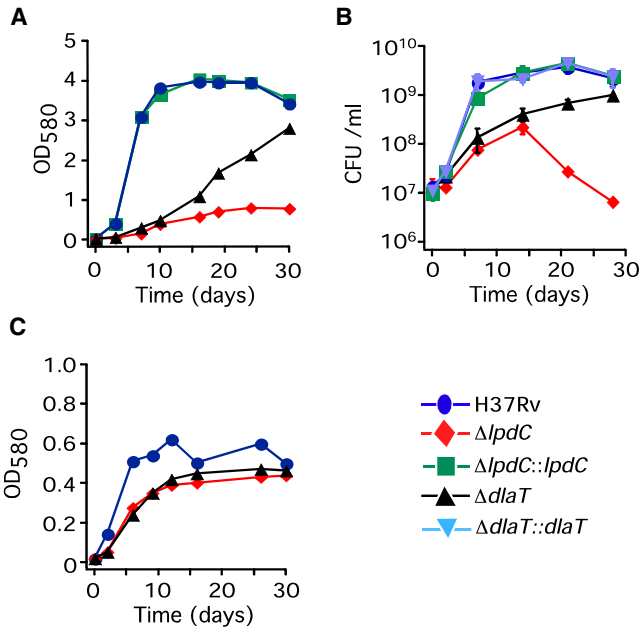


**Figure 3. Mtb Lacking *dlaT* Grows and Survives Better Than Mtb Lacking *lpdC***

(A) Growth of wild-type, mutants (Δ*lpdC*, Δ*dlaT*), and complemented strains (Δ*lpdC*::*lpdC*, Δ*dlaT*::*dlaT*) in complete 7H9 medium.

(B) Survival of the same strains as measured by change in CFUs. Means ± SD are shown of triplicate cultures.

(C) Growth in 7H9 containing no carbohydrate carbon sources. All results are representative of at least two independent experiments.

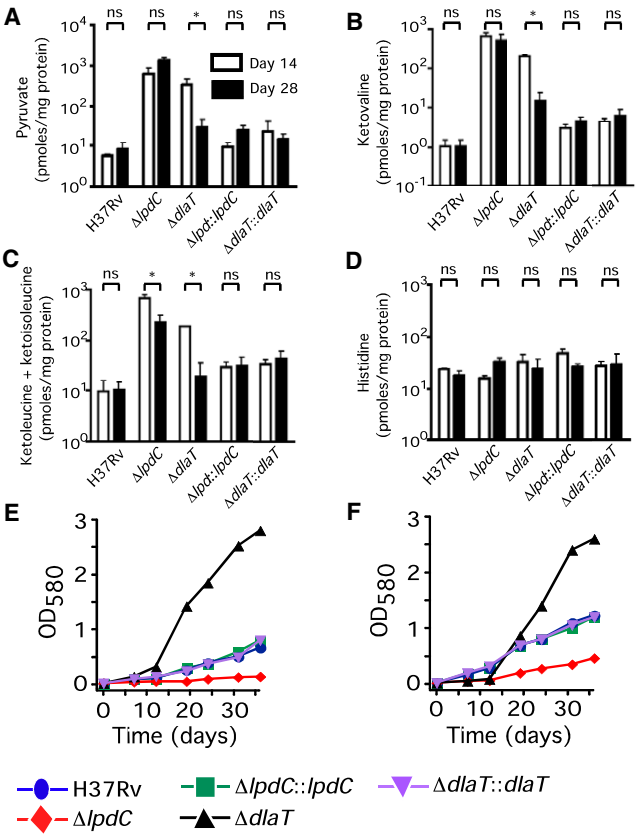


**Figure 4. Dysregulation of Intracellular Metabolite Pools in Wild-Type, Mutant, and Complemented Strains**

(A–D) Levels of intracellular pyruvate (A), ketovaline (B), ketoleucine + ketoisoleucine (C), and histidine (D) in wild-type, mutant, and complemented strains. Means ± SD for metabolite data of triplicate experimental samples are shown from one experiment, representative of two. *$p < 0.02$.

(E, F) Growth of strains in 7H9 medium containing 0.2% (w/v) leucine (E) or 0.2% (w/v) isoleucine (F) as the sole carbon sources. Growth curves are representative of at least three experiments.

also arise from pyruvate and their levels were also elevated at day 14 in both mutant strains compared to wild-type and complemented strains (see Figures S4B–S4D). Metabolism of branched-chain amino acids results in generation of branched-chain keto acids, which are direct substrates for the BCKADH complex. The intracellular levels of ketovaline, ketoleucine, and ketoisoleucine were similarly elevated in both mutant strains compared to wild-type and complemented strains (Figures 4B and 4C). In contrast, histidine, whose metabolism is independent of PDH, was equally abundant in all five strains (Figure 4D). At day 28, when the *dlaT* mutant had continued to grow but the *lpdC* mutant had stopped growing, intracellular pyruvate, leucine, isoleucine, valine, and their keto acid metabolites returned to near normal levels in the *dlaT* mutant, suggesting that they had been metabolized. However, these metabolites all remained elevated in Mtb lacking *lpdC* (Figures 4A–4C and Figures S4A–S4D), while histidine remained constant (Figure 4D). The reduction in levels of ketoleucine and/or ketoisoleucine in the *dlaT* mutant from day 14 to day 28 ($p = 0.0026$ for the difference between the two time points) brought the level nearly to that of the wild-type strain. In contrast, there was a much smaller reduction in levels in the *lpdC* mutant ($p = 0.01$ for the difference between the two time points). As noted, complementation of the mutant strains partially or completely restored levels of metabolites to wild-type levels (Figures 4A–4D and Figures S4A–S4D). Thus, early in culture, both DlaT-deficient Mtb and Lpd-deficient Mtb gave metabolic evidence of their PDH deficiency. However, between the second and fourth weeks of culture, the metabolic profile of DlaT-deficient Mtb and Lpd-deficient Mtb diverged. DlaT-deficient Mtb appeared to acquire the ability to overcome the block in metabolite flux, while Lpd-deficient Mtb did not.

Consistent with this, Mtb lacking DlaT grew on leucine (Figure 4E) and isoleucine (Figure 4F) even better than wild-type and complemented strains. In contrast, Mtb lacking Lpd was unable to grow on leucine or isoleucine. In this respect, Lpd-deficient Mtb phenocopied Mtb lacking both *Icl1* and *Icl2* (see Figures S4E and S4F). Thus, both Lpd and the methylcitrate cycle and/or glyoxylate shunt are required for growth on branched-chain amino acids. In contrast, absence of DlaT augmented the ability of Mtb to grow on these substrates, perhaps by forcing Mtb to express an Lpd-dependent enzyme that metabolizes them. Neither the mutants nor wild-type Mtb was able to grow on valine.

## Appearance of BCKADH in PDH-Deficient Mtb

To identify proteins that complex with Lpd in different circumstances, we generated Lpd tagged with octapeptide and hemagglutinin (FLAG-HA) and introduced it into both the *lpdC*

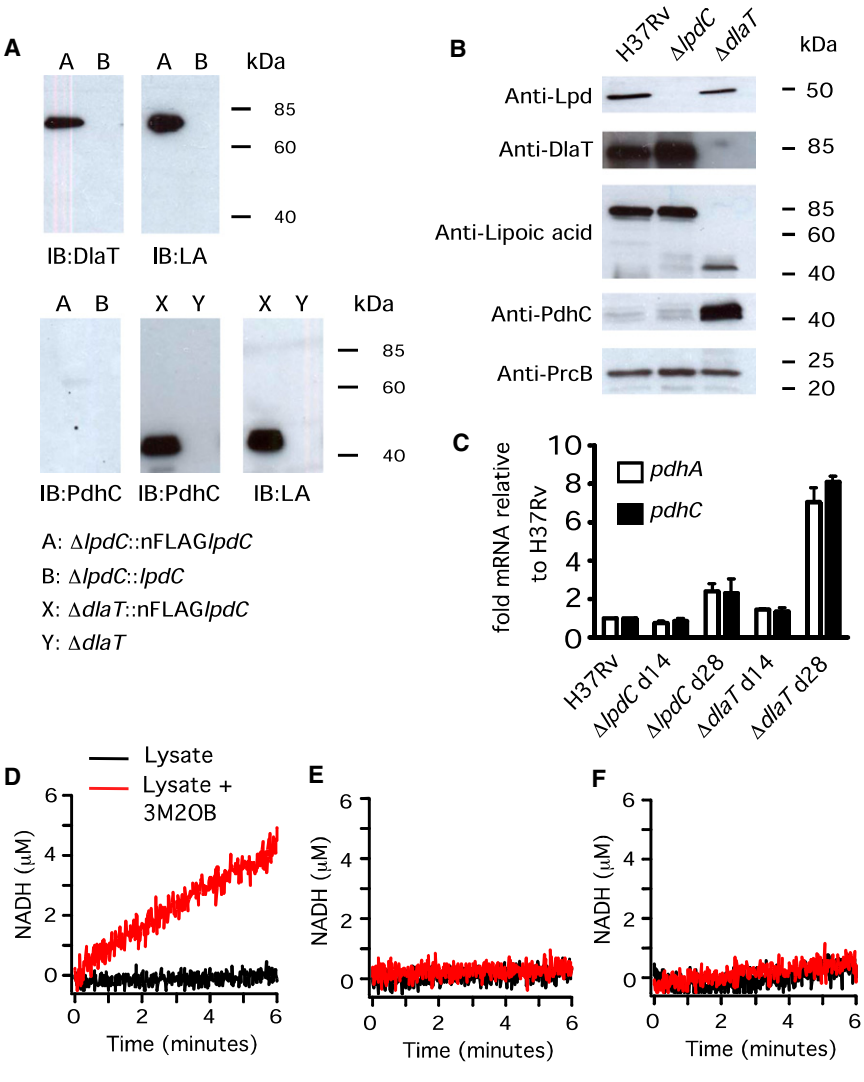


**Figure 5. Characterization of BCKADH Complex in Mtb**

(A) Immunoblot (IB) of the immunoprecipitate from the Δ*lpdC*::FLAG*lpdC* and the Δ*dlaT*::FLAG*lpdC* strains by using antisera against DlaT, lipoic acid (LA), and PdhC.

(B) Western blot of lysates from wild-type and mutant strains collected at day 28 postinoculation at $OD_{580}$ = 0.02 by using antisera against Lpd, DlaT, LA, PdhC, and PrcB, used as a loading control. Immunoprecipitations and western blots were performed at least twice.

(C) Levels of *pdhA* and *pdhC* transcripts assessed by qRT-PCR at indicated time points in wild-type and mutant strains. Results show means ± SD of one sample from three individual experiments, normalized to fold above *sigA*.

(D–F) In vitro BCKADH activity in lysates prepared from DlaT-deficient Mtb (D), wild-type Mtb (E), and Lpd-deficient Mtb (F). Results are representative of two experiments.

and *dlaT* mutants (Δ*lpdC*::FLAG*lpdC* and Δ*dlaT*::FLAG*lpdC*). FLAG-HA-tagged Lpd restored growth of the *lpdC* mutant in 7H9 medium to wild-type levels, suggesting that the tag did not interfere with Lpd's functional associations. Introduction of FLAG-HA-tagged Lpd into the *dlaT* mutant had no discernible effect on its growth (see Figure S5A). After 28 days of growth in 7H9 medium, we lysed the bacteria and immunoprecipitated Lpd with α-FLAG antibody. E2's of keto acid dehydrogenase complexes require lipoic acid as a prosthetic group (Perham, 2000). In earlier work, DlaT was the only lipoylated protein we could detect in wild-type Mtb (Bryk et al., 2002). In Δ*lpdC*::FLAG*lpdC*, DlaT was the major interacting partner of Lpd and was again the only lipoylated protein observed in the immunoprecipitate (Figure 5A). In contrast, in the Δ*dlaT*::FLAG*lpdC* strain, Lpd coimmunoprecipitated with PdhA, PdhB, and PdhC, as identified by peptide mass fingerprinting (see Table S1). An antibody we raised against pure, recombinant PdhC immunoblotted a protein in the latter immunoprecipitate that migrated at 42 kDa, as expected for PdhC. The anti-PdhC antibody reacted with nothing in a control immunoprecipitate prepared from lysates of Δ*dlaT* Mtb in which native LpdC did not carry the FLAG epitope (Figure 5A). The results with anti-PdhC antibody strongly reinforced the mass spectroscopic evidence that PdhC associates specifically with LpdC. Finally, in the anti-LpdC-FLAG immunoprecipitates from lysates of Δ*dlaT* Mtb, a protein distinct from DlaT became lipolyated and it comigrated with PdhC (Figure 5A).

Next, we monitored the status of protein lipoylation in the total lysates of Mtb strains rather than only in Lpd-interacting proteins, again focusing on 28 day cultures. In DlaT-deficient Mtb, we detected only one lipolylated protein. It migrated at ~42 KDa and comigrated with the upper band in the doublet immunoblotted by anti-PdhC (Figure 5B). The lower band in the doublet thus corresponds to PdhC that was not lipoylated. Although there was a nonlipoylated fraction of PdhC in Mtb lysates, the PdhC recovered from anti-Lpd immunoprecipitates migrated as a singlet (Figure 5A). These observations suggest that only lipoylated PdhC binds LpdC. In contrast, only DlaT was lipoylated in wild-type and Lpd-deficient Mtb. Moreover, the level of PdhC in DlaT-deficient Mtb appeared to be higher than in wild-type Mtb or Lpd-deficient Mtb. Consistent with this, transcripts for *pdhA* and *pdhC* were 8-fold higher in DlaT-deficient Mtb than in wild-type and Lpd-deficient strains (Figure 5C). Deep sequencing of the transcriptomes of wild-type and DlaT-deficient Mtb revealed that *pdhA*, *pdhB*, and *pdhC* were the most highly upregulated genes in the *dlaT* mutant, being expressed at levels 14.3-, 12.5- and 12.5-fold, respectively, higher than the levels in wild-type Mtb (R.B., unpublished observations). We amplified cDNA across the junctions of *pdhA-B* and *pdhB-C* and verified that *pdhABC* are transcribed as an operon (see Figure S5B).

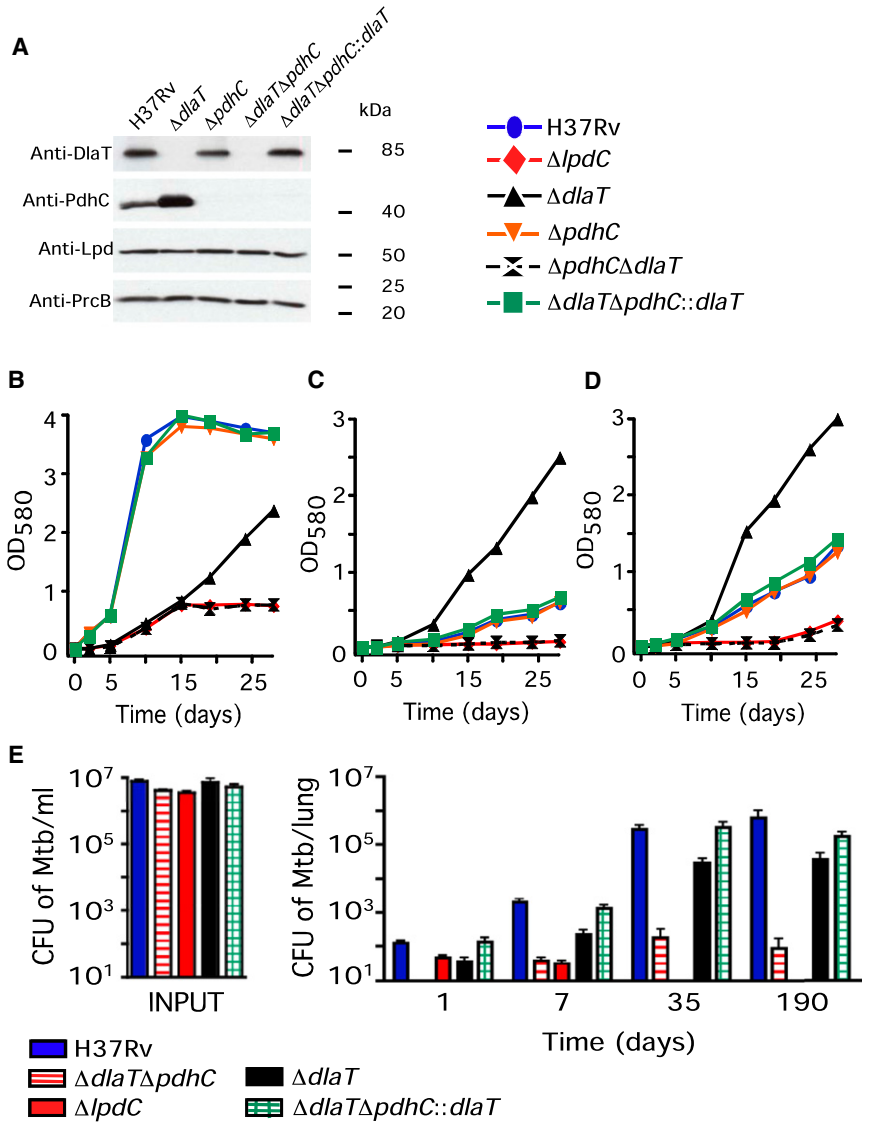


**Figure 6. Characterization of an Mtb Mutant Lacking Both *dlaT* and *pdhC***

(A) Western blot of wild-type, Δ*dlaT*, Δ*pdhC*, Δ*dlaT*Δ*pdhC*, and the complemented strain (Δ*dlaT*Δ*pdhC*::*dlaT*) was performed by using antisera against DlaT, PdhC, Lpd, and PrcB.

(B–D) Growth curve of the above strains as well as Mtb lacking *lpdC,* in complete 7H9 medium (B), medium containing leucine (C), or medium containing isoleucine (D) as the sole carbon source.

(E) Survival of wild-type, Δ*dlaT*Δ*pdhC*, Δ*lpdC*, Δ*dlaT*, and Δ*dlaT*Δ*pdhC*::*dlaT* strains in lungs of C57BL/6 mice infected via aerosol. Means ± SD for four mice per Mtb strain are shown from one experiment, representative of at least two.

Finally, BCKADH activity was evident in lysates from 28 day cultures of DlaT-deficient Mtb with 3-methyl 2-oxobutyrate (3M2OB) as a substrate (Figure 5D). Lysates from wild-type, Lpd-deficient, and DlaT-complemented strains showed no BCKADH activity (Figures 5E and 5F and Figure S5C). Lysates from 14 day wild-type and Δ*lpdC* cultures lacked BCKADH activity, while lysates from 14 day Δ*dlaT* cultures showed very low levels of BCKADH activity (see Figure S5D). As a control, we also measured PDH activity in wild-type and mutant lysates. As expected, only the wild-type strain carried out this reaction (see Figure S5E).

Thus, in the absence of DlaT, Mtb upregulated *pdhABC*, expressed readily detectable quantities of lipoylated PdhC in complex with Lpd, and acquired the ability to metabolize branched-chain keto acids.

## Recapitulation of Lpd Deficiency by Double Deficiency of DlaT and PdhC

To help confirm the foregoing interpretations, we deleted *pdhC* from H37Rv, generating Δ*pdhC*, and from H37RvΔ*dlaT*, generating Δ*dlaT*Δ*pdhC*. We confirmed the disruption of *pdhC* by western (Figure 6A) and Southern blotting and qRT-PCR (see Figures S6A and S6B). The strain Δ*dlaT*Δ*pdhC* was severely attenuated in its ability to grow in 7H9 containing glycerol and dextrose, as well as on leucine or isoleucine, thus phenocopying Δ*lpdC*. The strain lacking only PdhC did not appear to have a growth defect in any of these conditions, suggesting that when PdhC is missing, these substrates may be metabolized via PDH. Only when the E2's of PDH and BCKADH were both missing did it appear that glycolytic and branched-chain carbon sources could no longer be metabolized. Introduction of a single copy of the *dlaT* gene into Δ*dlaT*Δ*pdhC*, generating Δ*dlaT*Δ*pdhC*::*dlaT*, complemented all growth phenotypes to wild-type levels (Figures 6B–6D).

Finally, we infected C57BL/6 mice with both the Δ*pdhC* and the Δ*dlaT*Δ*pdhC* mutants. As controls, we also infected mice with Δ*dlaT*Δ*pdhC*::*dlaT*, Δ*lpdC*, or Δ*dlaT*. The Δ*pdhC* mutant resembled wild-type Mtb (see Figure S6C) in its virulence. Reproducibly, the Δ*dlaT*Δ*pdhC* strain could not be recovered at day 1, despite equal input into the aerosolizer. However, by day 7, the Δ*dlaT*Δ*pdhC* and Δ*lpdC* mutants were both recovered at ~100 CFUs. This suggests that the Δ*dlaT*Δ*pdhC* mutant was viable but nonculturable at day 1 for unknown reasons. At day 35, the Δ*lpdC* strain could no longer be recovered. At that point, and at day 190, the Δ*dlaT*Δ*pdhC* mutant was 2–3 log more attenuated than the Δ*dlaT* mutant but more virulent than the Δ*lpdC* mutant. Complementation of the double knockout with *dlaT* restored wild-type virulence levels (Figure 6E). Thus, both PDH and BCKADH complexes are jointly required for virulence of Mtb. However, the finding that the Δ*dlaT*Δ*pdhC* mutant was not as attenuated as the Δ*lpdC* mutant suggests Lpd may play a fourth important role over and above its contributions to PDH, BCKADH, and PNR/P.

## DISCUSSION

This work sheds light on three facets of our understanding of host-pathogen interactions in experimental tuberculosis: how we assess the nutritional composition of the host niche; how a pathogen adapts to nutritional challenges; and how targets are validated in the search for anti-infectives that hold promise to be effective against Mtb in the host.

One major avenue in the study of host-pathogen relationships is to infer the properties of the pathogen's survival and growth niches in the host by assessing the phenotype of the pathogen when specific enzymes have been knocked out. Attenuation by knockout of a metabolic enzyme is often interpreted to mean that the pathogen must subsist in the host on that enzyme's substrate(s). This line of reasoning requires two key inputs: an accurate understanding of what reactions the enzyme catalyzes, which may be different from what was expected; and an assessment of whether the phenotype may reflect not lack of the enzyme's products, but rather, intoxication by substrates that accumulate in its absence. The extent to which metabolic substrates will actually accumulate in the absence of a given enzyme is difficult to predict. Most metabolites lie on multiple enzymatic pathways. We have insufficient knowledge of alternative pathways and their rate constants, particularly in the setting where one major route is inactivated and others may then be adaptively modulated, not only by transcription but also by changes in negative and positive feedback by substrates and products.

For example, Mtb is severely attenuated in the mouse by combined inactivation of *icl1* and *icl2* (Munoz-Elias and McKinney, 2005). While this was initially interpreted as reporting that Mtb subsists in vivo on fatty acids, subsequent in vitro studies with mutants of *M. smegmatis* cultured on various carbon sources led to an alternative interpretation, that poor survival of Mtb lacking Icl1 and Icl2 may reflect intoxication by accumulation of propionate and its metabolites (Upton and McKinney, 2007). That disruption of a gene encoding an enzyme can prove lethal from accumulation of toxic precursors was recently demonstrated for the Mtb maltosyltransferase encoded by *glgE* (Kalscheuer et al., 2010). Similarly, Pethe et al. identified pyrimidine imidazoles that killed Mtb in vitro by promoting accumulation of glycerol phosphate in a standard growth medium containing glycerol (Pethe et al., 2010).

Although Mtb requires leucine to survive, excess leucine in the growth medium proved toxic (data not shown). This is reminiscent of maple syrup urine disease, an autosomal recessive disorder of humans in which insufficiency of BCKADH leads to accumulation of toxic levels of branched-chain amino keto acids (Mackenzie and Woolf, 1959). In the present work, disruption of *lpdC* led to extraordinary accumulations of pyruvate and branched-chain amino and keto acids. These accumulations may cause this strain's marked attenuation. Metabolomic analysis was invaluable for allowing us to recognize this possibility. Thus, the first implication of our findings is that metabolomic analysis provides an important complement to gene knockout studies in research aimed at inferring the nutritional composition of the pathogen's niche in the host.

Another fundamental goal of studying host-pathogen interactions is to understand the molecular basis of the pathogen's adaptability to changing conditions. Adaptability is critical to pathogenesis, both when the pathogen changes niches upon infecting a new host and when the host responds to infection in ways that alter the niche. The present work has demonstrated a remarkably slow, extremely specific and functionally important adaptation by Mtb that consists in switching lipoylation from one protein substrate to an alternative protein substrate. Thus, when the E2 of PDH was genetically deleted, Mtb upregulated *pdhABC*, accumulated lipolyated PdhC, and expressed a BCKADH whose function was evident in the distribution of metabolites and the activity of lysates. In light of these findings, Rv2497c, Rv2496c, and Rv2495c can be reannotated as *bkdA*, *bkdB*, and *bkdC*, respectively. In contrast, wild-type and Lpd-deficient Mtb grown on a standard rich medium in vitro either did not express a functional BCKADH complex or expressed it at levels below our ability to detect it.

Yet another important goal of studying host-pathogen interactions is to guide the development of anti-infectives that are effective in vivo because they cripple pathways on which the pathogen actually depends in vivo. This has been difficult to predict from studies in vitro. A pathway can be essential in vitro but not in vivo (Pethe et al., 2010), or essential in vivo but not in vitro (Munoz-Elias and McKinney, 2005). Thus, it is important to learn that Δ*lpdC* Mtb was markedly attenuated in vivo. This could not have been predicted from our limited understanding of central carbon metabolism in Mtb.

It has commonly been thought that intermediary metabolism in Mtb mirrors that in other organisms and is therefore well understood. In fact, Mtb's core intermediary metabolism diverges markedly from the standard model. For example, the tricarboxylic acid cycle is interrupted by the lack of αKGDH (Tian et al., 2005b). A unique anaerobic-type but aerobically active ferredoxin oxidoreductase acts on α-ketoglutarate (Baughn et al., 2009) but metabolomic analysis does not support the interpretation that the oxidative and reductive arms of the tricarboxylic acid cycle are fully joined (de Carvalho et al., 2010a, 2010b). Additionally, the pentose-phosphate pathway and tricarboxylic acid cycle in Mtb are extensively compartmentalized from each other (de Carvalho et al., 2010a. In short, core intermediary metabolism in Mtb is vitally important but incompletely understood. Combining the tools of genetics, biochemistry, metabolomics, and infections can help fill this gap.

We were surprised to discover that Mtb was more attenuated by lack of Lpd than by lack of DlaT or even by lack of both DlaT and PdhC. Lpd clearly has important functions that it does not share with DlaT. At present, participation in BCKADH is the only such function identified. Transcription of *bkdABC* was detected in Mtb recovered from lungs of mice but only at the same low level as in Mtb grown in rich medium in vitro (Talaat et al., 2004). This leaves open the question whether BCKADH is expressed at the protein level to an extent that can contribute to the metabolism of PDH-replete Mtb during infection of the mouse or only plays a role when it is upregulated, for example, in the context of insufficient PDH activity. In either setting, BCKADH might be critical to Mtb's survival for several reasons. Above, we stressed the role of BCKADH in avoiding accumulation of pyruvate, branched-chain amino acids, and branched-chain keto acids. Additionally or alternatively, in glucose-limiting conditions in vivo, Mtb may operate a phosphoenol pyruvate

(PEP)-glyoxylate pathway, whose activity is dependent on PDH (Fischer and Sauer, 2003; Munoz-Elias and McKinney, 2006). In the absence of PDH, BCKADH may be able to shunt metabolites from pyruvate to acetyl coA, as is required for the functioning of the PEP-glyoxylate pathway. In vitro, carbon-starved Mtb upregulated transcripts for *bkdA*, *bkdB*, *bkdC*, and *icl1* (Betts et al., 2002). Thus, when otherwise facing starvation, Mtb may metabolize branched-chain keto and amino acids via BCKADH as a source of energy. Finally, BCKADH may help regulate the levels of branched-chain lipids. Inactivation of the BCKADH complex in *Staphylococcus aureus* and *Myxococcus xanthus* led to a decrease in quantity of branched-chain fatty acids in the cell membrane and rendered the mutants more susceptible to a variety of stresses (Singh et al., 2008; Toal et al., 1995). Changes in Mtb's branched-chain fatty acids likewise affect Mtb's virulence (Glickman and Jacobs, 2001). Thus, the present work establishes the contribution of LpdC to BCKADH in Mtb and the essentiality of LpdC for Mtb's virulence in the mouse. However, it is not yet clear how BCKADH contributes to Mtb's virulence.

The essentiality of mycobacterial Lpd in the mouse and the participation of this one protein in at least three different enzyme complexes (Figure 7) suggest that Lpd might be a promising target for chemotherapy of tuberculosis. The triazospirodimethoxybenzoyl inhibitor that inhibits Mtb's Lpd while sparing human Lpd was not able to enter intact Mtb but its identification demonstrates that species-selective Lpd inhibition is attainable (Bryk et al., 2010).

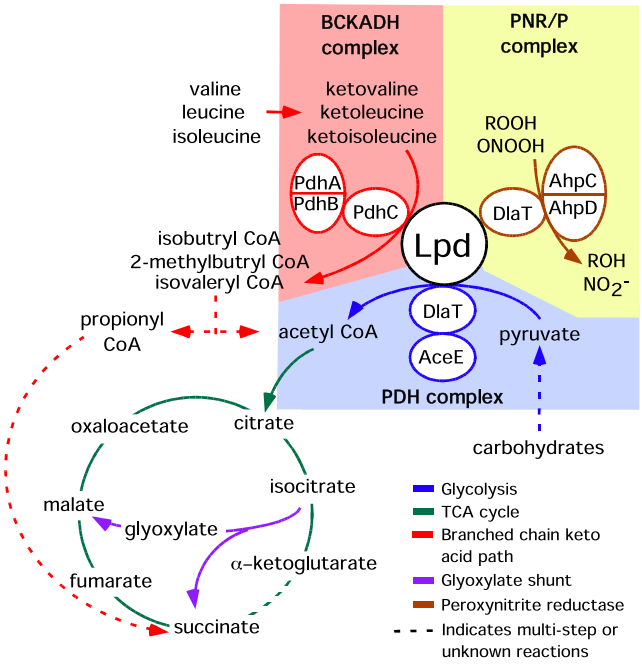


**Figure 7. Schematic Showing Roles of Lpd in PDH, BCKADH, and PNR/P Complexes in Mtb**

## EXPERIMENTAL PROCEDURES

### Strains and Culture Conditions

Wild-type Mtb H37Rv, mutants, and complemented strains were cultured at 37°C in Middlebrook 7H9 with 0.2% glycerol, 0.5% bovine serum albumin fraction V (BSA), 0.05% Tween 80, 0.2% dextrose, and 0.085% NaCl (standard medium). Studies on defined carbon sources (0.2%) used fatty acid-stripped BSA (Roche) without glycerol and dextrose with tyloxapol (0.02%) and vitamin B12 (10 μg/ml) (Savvi et al., 2008). CFUs were determined on 7H11 agar plates after 4 weeks at 37°C. Strains bearing antibiotic resistance cassettes were cultured in the presence of hygromycin (50 μg/ml), kanamycin (30 μg/ml), streptomycin (30 μg/ml), or zeocin (25 μg/ml). For growth on solid medium, Middlebrook 7H11 was supplemented with 0.5% glycerol and 10% oleic acid-dextrose-catalase (7H11-OADC).

### Mutant Strains

Efforts to delete *lpdC* (Rv0462, *lpdC*) from the genome of Mtb H37Rv were initially unsuccessful. We cloned *lpdC* into an integrative complementation vector (pMV306k) downstream of a constitutively active hsp60 promoter. pMV306k-hsp60*lpdC* was transformed into wild-type H37Rv to create a merodiploid strain carrying *lpdC* at its native site as well as at the *attB* site (H37Rv::*lpdC*). *LpdC* was deleted from the native site of the H37Rv merodiploid strain via a single-step recombination with the mycobacteriophage pHAE87 (Bardarov et al., 1997). Five hundred and fifty base pairs (bp) upstream and 500 bp downstream of *lpdC* were cloned into the plasmid pJSC284 flanking a hygromycin resistance cassette. The recombinant mycobacteriophage was used to infect H37Rv::*lpdC*. Knockout colonies were screened by PCR and confirmed by Southern blotting. The complementing plasmid was switched out of the *attB* site with an empty plasmid bearing a streptomycin resistance cassette, pTCS-mcs1, creating H37RvΔ*lpdC* pTCS-mcs1 (H37RvΔ*lpdC*).

To construct FLAG-HA tagged *lpdC*, we fused an N-terminal FLAG-HA tag (codon optimized for use in Mtb) to *lpdC* by PCR, deleting the N-terminal valine of Lpd (FLAG-Lpd). This was cloned into an episomal plasmid, pTEK-hsp60, downstream of the hsp60 promoter. pTEK hsp60 nFLAG-HA*lpdC* was transformed into H37RvΔ*lpdC* (Δ*lpdC*::FLAG*lpdC*) and H37RvΔ*dlaT* (Δ*dlaT*::FLAG*lpdC*).

*PdhC* (Rv2495c) was deleted via single-step recombination by using the mycobacteriophage pHAE87 with a streptomycin resistance cassette. Regions flanking *pdhC* (727 bp upstream, 717 bp downstream) were cloned on either side of the streptomycin cassette. The recombinant mycobacteriophage infected H37Rv and H37RvΔ*dlaT*::*dlaT*, creating H37RvΔ*pdhC* and H37RvΔ*pdhC*Δ*dlaT*::*dlaT*. Colonies were screened by PCR and confirmed by Southern blotting. To create a strain lacking both DlaT and PdhC, we switched the complementing plasmid out of the *attB* site of H37RvΔ*pdhC*Δ*dlaT*::*dlaT* with an empty plasmid bearing a zeocin resistance cassette, pTCZ-MCS1, creating H37RvΔ*pdhC*Δ*dlaT* pTCZ-mcs1 (Δ*pdhC*Δ*dlaT*).

To confirm deletion of *lpdC*, we digested genomic DNA from wild-type H37Rv and knockout candidates with XmaI and NcoI, separated it by agarose gel electrophoresis, and transferred it to a nylon membrane that was probed with a 500-bp digoxygenin-labeled fragment containing the upstream *lpdC* 5′ flanking fragment, revealing a 4.5 kb band for wild-type Mtb and a 2.7 kb band for *lpdC*-deficient Mtb.

Genomic DNA from H37RvΔ*pdhC* and H37RvΔ*pdhC*Δ*dlaT*::*dlaT* was digested with EcoRV and XmaI and transferred to a nylon membrane that was probed with a fragment containing 300 bp of *pdhB* yielding a 1.5 kb fragment for wild-type and a 3.5 kb fragment for *pdhC*-deficient Mtb upon Southern blotting with the ECL Direct Nucleic Acid Labeling and Detection System (Amersham).

### Antisera to Lpd and PdhC

Recombinant Lpd purified as reported (Argyrou and Blanchard, 2001) was used to immunize chickens. Recombinant PdhC purified as reported (Tian et al., 2005b) was used to immunize rabbits.

### Stress Assays

For nitrosative stress, Mtb strains were grown to mid-log phase and washed twice in 7H9 acidified to pH 5.5 with HCl. Cultures were centrifuged at 120 *g* for 10 min to remove clumps. Supernatants were adjusted to an $OD_{580}$ = 0.1, $NaNO_2$ was added, and CFUs were determined after 4 days. For oxidative stress, Mtb strains prepared as above but in nonacidified medium were

adjusted to an $OD_{580}$ = 0.1, $H_2O_2$ was added, and CFUs were determined after 4 hr. For other stresses, Mtb strains prepared as above were adjusted to $OD_{580}$ = 0.1 and SDS or antibiotics were added. CFUs were determined after 1 hr with SDS and after 4 hr with lipophilic antibiotics. All experiments were performed in triplicate with serial dilution and plating on 7H11 agar, counting CFUs after 4 weeks at 37°C.

### Mouse Infections

C57BL/6 wild-type and IFN$\gamma^{-/-}$ mice (Jackson Labs) were infected by using an Inhalation Exposure System (Glas-Col). Early to mid-log phase Mtb was washed once in PBS + 0.05% Tween 80 (PBST) and centrifuged at 120 *g* to remove clumps. The inoculum (6 ml, adjusted to an $OD_{580}$ = 0.002–0.005) was nebulized for 40 min. Lungs and spleen were homogenized in PBS, serially diluted, and plated on 7H11 agar. For mice infected with Lpd-deficient or DlaT/PdhC-deficient Mtb, entire organ homogenates were plated on 7H11-OADC plates, except in mice euthanized on days 64 and 164, in which the upper left lobe was reserved for histology. Plates were incubated at 37°C for 5 weeks if no CFUs were detected earlier. In most experiments, the upper lobe of the left lung was fixed in 4% paraformaldehyde for histopathology.

### Macrophage Infections

Marrow cells were flushed from femurs of 8- to 10-week-old C57BL/6 mice and incubated for 6 days at 37°C, 5% $CO_2$ in Dulbecco's modified Eagle's medium (DMEM) (GIBCO) with 10% heat-inactivated fetal calf serum, 20% L929 fibroblast-conditioned medium, 1 mM sodium pyruvate (Mediatech Inc.), 10 mM HEPES (GIBCO), and 0.58 g/L L-glutamine (Mediatech Inc.). Cells were fed with the same medium at day 4 and seeded in 48-well plates on day 6 (Ehrt et al., 2001). Where indicated, macrophages were stimulated with IFN$\gamma$ (10 ng/ml, R&D Systems). Mid-log Mtb cultures were washed twice in PBST. Clumps were removed by centrifugation at 120 *g* and the macrophages were infected with 0.1 Mtb per macrophage. CFUs were assessed over a period of 6 days (Ehrt et al., 2001).

### Quantitative Real-Time PCR

We grew Mtb in standard medium starting at an $OD_{580}$ of 0.05 for 14 and 28 days and added an equal volume of buffer containing guanidinium thiocyanate (4 M), sodium lauryl sulfate (0.5%), trisodium citrate (25 mM), and 2-mercaptoethanol (0.1 M). Cultures were pelleted, resuspended in TRIzol, and bead-beaten three times. RNA was extracted and qRT-PCR was performed by using gene-specific Taqman probes and primers (Biosearch Technologies).

### Analysis of Intracellular Metabolites

Mtb was grown to mid-log phase in standard medium and diluted to an $OD_{580}$ of 0.2. One milliliter of each culture was filtered through a nitrocellulose membrane (0.22 μM, Millipore GSWP 02500). Mtb-bearing filters were placed on individual 7H9 agar plates supplemented with 0.5% glycerol, 0.5% BSA, 0.2% dextrose, and 0.085% NaCl with the bacterial surface on top. Plates were incubated at 37°C in 5% $CO_2$ for 14 and 28 days. Filters were flipped onto a 1 ml ice-cold solution of 40% acetonitrile, 40% methanol, and 20% water. Bacteria were scraped off the filter and lysed by bead-beating three times. Intracellular metabolites and those that had leaked into the lysis solution were pooled as described (de Carvalho et al., 2010a, 2010b). Metabolite abundances were quantified by using a calibration curve generated with chemical standards spiked into homologous mycobacterial extracts to correct for matrix-associated ion-suppression effects. Protein was measured by using the Bio-Rad DC assay (Bio-Rad). Ion counts of specific metabolites were normalized to total protein. Statistical significance was assessed with the Mann-Whitney t test ($p < 0.02$).

### Immunoblotting and Immunoprecipitation

Mtb was grown to late stationary phase (28 days in culture) in standard medium, pelleted, washed twice in PBST, and resuspended in potassium phosphate buffer (KPi, 25 mM) containing EDTA (1 mM) and phenylmethanesulfonyl fluoride (PMSF) (1 mM). Lysates were prepared by bead-beating three times and pelleting at 20,000 *g*. Proteins (15–30 μg) were separated by SDS-PAGE and transferred to a nitrocellulose membrane. Antisera used were anti-Lpd (1:5000); anti-PdhC (1:5000); anti-DlaT (1:10,000) (Bryk et al., 2002); anti-proteasome component B (PrcB) (1:10,000) (Gandotra et al., 2007); or anti-lipoic acid (Calbiochem, 1:2500). Secondary antibodies used were rabbit anti-chicken immunoglobulin Y (Promega, 1:5000) and donkey anti-rabbit IgG (Amersham, 1:10,000). Lysates of late log-phase cultures of Δ*lpdC*::FLAG*lpdC*, Δ*dlaT*::FLAG*lpdC*, H37Rv, and H37RvΔ*dlaT* were adjusted to 5 mg/ml with the lysis buffer, precleared with Sepharose beads for 1 hr, and incubated with anti-FLAG M2 beads (SIGMA) at 4°C overnight. Beads were washed three times with wash buffer (WB300) containing Tris, pH 7.4 (20 mM), NaCl (300 mM), glycerol (10%), EDTA (0.2 mM), Triton X-100 (0.2%), PMSF (1 mM), and dithiothreitol (1 mM). The beads were then washed with WB100 buffer containing only 100 mM NaCl and eluted in WB100 containing 2xFLAG peptide (SIGMA) for SDS-PAGE and western blotting.

### Enzyme Assays

Lysates of late log-phase cultures (1 mg protein/ml) were incubated in cuvettes at 37°C in KPi (25 mM) with oxidized nicotinamide adenine dinucleotide (1 mM), thiamine pyrophosphate (0.2 mM), coA (0.17 mM), MgCl (1 mM), and 3M2OB (2 mM) (Fluka). Production of reduced nicotinamide adenine dinucleotide was monitored at 340 nm in a Uvikon XL spectrophotometer.

## SUPPLEMENTAL INFORMATION

Supplemental Information includes six figures and one table and can be found with this article online at doi:10.1016/j.chom.2010.12.004.

## ACKNOWLEDGMENTS

We thank Xuiju Jiang, Jean Schneider, Charlie G. Buffie, and Sheetal Gandotra for assistance; Luiz Pedro Sorio De Carvalho for anti-PdhC antiserum, John McKinney for the Δ*icl*1/2 strain, and Haiqiang Yu and Haiteng Deng of the Rockefeller University Mass Spectrometry Core facility for mass spectrometric analysis. The authors declare no competing financial interests. This study was supported by National Institutes of Health (NIH) RO1 AI064768. K.R. is supported by a Burroughs Wellcome Career Award in the Biomedical Sciences, the William Randolph Hearst Foundation Clinical Scholar Award, and NIH R21 AI081094. The Department of Microbiology and Immunology of Weill Cornell Medical College is supported by the William Randolph Hearst Foundation. A.V. designed and performed experiments, analyzed data, and prepared figures. R.B. and P.R. helped with experiments. S.S. and S.E. constructed the *lpd* mutant bacteria. D.S. provided constructs and advice. K.R. helped with metabolomic experiments. C.N. guided the study. A.V. and C.N. wrote the article. All authors discussed results and commented on the manuscript.

Received: May 7, 2010
Revised: October 18, 2010
Accepted: December 1, 2010
Published: January 19, 2011

## REFERENCES

Argyrou, A., and Blanchard, J.S. (2001). *Mycobacterium tuberculosis* lipoamide dehydrogenase is encoded by Rv0462 and not by the lpdA or lpdB genes. Biochemistry *40*, 11353–11363.

Bardarov, S., Kriakov, J., Carriere, C., Yu, S., Vaamonde, C., McAdam, R.A., Bloom, B.R., Hatfull, G.F., and Jacobs, W.R., Jr. (1997). Conditionally replicating mycobacteriophages: a system for transposon delivery to *Mycobacterium tuberculosis*. Proc. Natl. Acad. Sci. USA *94*, 10961–10966.

Barry, C.E., 3rd, Boshoff, H.I., Dartois, V., Dick, T., Ehrt, S., Flynn, J., Schnappinger, D., Wilkinson, R.J., and Young, D. (2009). The spectrum of latent tuberculosis: rethinking the biology and intervention strategies. Nat. Rev. Microbiol. *7*, 845–855.

Baughn, A.D., Garforth, S.J., Vilcheze, C., and Jacobs, W.R., Jr. (2009). An anaerobic-type alpha-ketoglutarate ferredoxin oxidoreductase completes the oxidative tricarboxylic acid cycle of *Mycobacterium tuberculosis*. PLoS Pathog. *5*, e1000662.

Betts, J.C., Lukey, P.T., Robb, L.C., McAdam, R.A., and Duncan, K. (2002). Evaluation of a nutrient starvation model of *Mycobacterium tuberculosis*

persistence by gene and protein expression profiling. Mol. Microbiol. *43*, 717–731.

Bloom, B.R., and Murray, C.J. (1992). Tuberculosis: commentary on a reemergent killer. Science *257*, 1055–1064.

Bryk, R., Griffin, P., and Nathan, C. (2000). Peroxynitrite reductase activity of bacterial peroxiredoxins. Nature *407*, 211–215.

Bryk, R., Lima, C.D., Erdjument-Bromage, H., Tempst, P., and Nathan, C. (2002). Metabolic enzymes of mycobacteria linked to antioxidant defense by a thioredoxin-like protein. Science *295*, 1073–1077.

Bryk, R., Gold, B., Venugopal, A., Singh, J., Samy, R., Pupek, K., Cao, H., Popescu, C., Gurney, M., Hotha, S., et al. (2008). Selective killing of nonreplicating mycobacteria. Cell Host Microbe *3*, 137–145.

Bryk, R., Arango, N., Venugopal, A., Warren, J.D., Park, Y.H., Patel, M.S., Lima, C.D., and Nathan, C. (2010). Triazaspirodimethoxybenzoyls as selective inhibitors of mycobacterial lipoamide dehydrogenase. Biochemistry *49*, 1616–1627.

Chan, E.D., Strand, M.J., and Iseman, M.D. (2008). Treatment outcomes in extensively resistant tuberculosis. N. Engl. J. Med. *359*, 657–659.

Cole, S.T., and Barrell, B.G. (1998). Analysis of the genome of *Mycobacterium tuberculosis* H37Rv. Novartis Found. Symp. *217*, 160–172, discussion 172–177.

Darwin, K.H., Ehrt, S., Gutierrez-Ramos, J.C., Weich, N., and Nathan, C.F. (2003). The proteasome of *Mycobacterium tuberculosis* is required for resistance to nitric oxide. Science *302*, 1963–1966.

de Carvalho, L.P., Fischer, S.M., Marrero, J., Nathan, C., Ehrt, S., and Rhee, K.Y. (2010a). Metabolomics of *Mycobacterium tuberculosis* reveals compartmentalized co-catabolism of carbon substrates. Chem. Biol. *17*, 1122–1131.

de Carvalho, L.P.S., Zhao, H., Dickinson, C.E., Arango, N.M., Lima, C.D., Fischer, S.M., Ouerfelli, O., Nathan, C., and Rhee, K.Y. (2010b). Activity-based metabolomic profiling of enzymatic function: Identification of Rv1248c as a mycobacterial 2-hydroxy-3-oxoadipate synthase. Chem. Biol. *17*, 323–332.

Ehrt, S., Schnappinger, D., Bekiranov, S., Drenkow, J., Shi, S., Gingeras, T.R., Gaasterland, T., Schoolnik, G., and Nathan, C. (2001). Reprogramming of the macrophage transcriptome in response to interferon-gamma and *Mycobacterium tuberculosis*: signaling roles of nitric oxide synthase-2 and phagocyte oxidase. J. Exp. Med. *194*, 1123–1140.

Fischbach, M.A., and Walsh, C.T. (2009). Antibiotics for emerging pathogens. Science *325*, 1089–1093.

Fischer, E., and Sauer, U. (2003). A novel metabolic cycle catalyzes glucose oxidation and anaplerosis in hungry *Escherichia coli*. J. Biol. Chem. *278*, 46446–46451.

Flynn, J.L., Chan, J., Triebold, K.J., Dalton, D.K., Stewart, T.A., and Bloom, B.R. (1993). An essential role for interferon gamma in resistance to *Mycobacterium tuberculosis* infection. J. Exp. Med. *178*, 2249–2254.

Gandotra, S., Schnappinger, D., Monteleone, M., Hillen, W., and Ehrt, S. (2007). In vivo gene silencing identifies the *Mycobacterium tuberculosis* proteasome as essential for the bacteria to persist in mice. Nat. Med. *13*, 1515–1520.

Gill, W.P., Harik, N.S., Whiddon, M.R., Liao, R.P., Mittler, J.E., and Sherman, D.R. (2009). A replication clock for *Mycobacterium tuberculosis*. Nat. Med. *15*, 211–214.

Glaziou, P., Floyd, K., and Raviglione, M. (2009). Global burden and epidemiology of tuberculosis. Clin. Chest Med. *30*, 621–636.

Glickman, M.S., and Jacobs, W.R., Jr. (2001). Microbial pathogenesis of *Mycobacterium tuberculosis*: dawn of a discipline. Cell *104*, 477–485.

Hondalus, M.K., Bardarov, S., Russell, R., Chan, J., Jacobs, W.R., Jr., and Bloom, B.R. (2000). Attenuation of and protection induced by a leucine auxotroph of *Mycobacterium tuberculosis*. Infect. Immun. *68*, 2888–2898.

Jouanguy, E., Altare, F., Lamhamedi-Cherradi, S., and Casanova, J.L. (1997). Infections in IFNGR-1-deficient children. J. Interferon Cytokine Res. *17*, 583–587.

Kalscheuer, R., Syson, K., Veeraraghavan, U., Weinrick, B., Biermann, K.E., Liu, Z., Sacchettini, J.C., Besra, G., Bornemann, S., and Jacobs, W.R., Jr. (2010). Self-poisoning of *Mycobacterium tuberculosis* by targeting GlgE in an alpha-glucan pathway. Nat. Chem. Biol. *6*, 376–384.

Mackenzie, D.Y., and Woolf, L.I. (1959). Maple syrup urine disease; an inborn error of the metabolism of valine, leucine, and isoleucine associated with gross mental deficiency. BMJ *1*, 90–91.

MacMicking, J., Xie, Q.W., and Nathan, C. (1997). Nitric oxide and macrophage function. Annu. Rev. Immunol. *15*, 323–350.

McCune, R.M., Feldmann, F.M., Lambert, H.P., and McDermott, W. (1966). Microbial persistence. I. The capacity of tubercle bacilli to survive sterilization in mouse tissues. J. Exp. Med. *123*, 445–468.

Munoz-Elias, E.J., and McKinney, J.D. (2005). *Mycobacterium tuberculosis* isocitrate lyases 1 and 2 are jointly required for in vivo growth and virulence. Nat. Med. *11*, 638–644.

Munoz-Elias, E.J., and McKinney, J.D. (2006). Carbon metabolism of intracellular bacteria. Cell. Microbiol. *8*, 10–22.

Munoz-Elias, E.J., Timm, J., Botha, T., Chan, W.T., Gomez, J.E., and McKinney, J.D. (2005). Replication dynamics of Mycobacterium tuberculosis in chronically infected mice. Infect. Immun. *73*, 546–551.

Nathan, C. (2009). Taming tuberculosis: a challenge for science and society. Cell Host Microbe *5*, 220–224.

Nathan, C., Gold, B., Lin, G., Stegman, M., de Carvalho, L.P., Vandal, O., Venugopal, A., and Bryk, R. (2008). A philosophy of anti-infectives as a guide in the search for new drugs for tuberculosis. Tuberculosis (Edinb.) *88* (*Suppl 1*), S25–S33.

Pandey, A.K., and Sassetti, C.M. (2008). Mycobacterial persistence requires the utilization of host cholesterol. Proc. Natl. Acad. Sci. USA *105*, 4376–4380.

Perham, R.N. (2000). Swinging arms and swinging domains in multifunctional enzymes: catalytic machines for multistep reactions. Annu. Rev. Biochem. *69*, 961–1004.

Pethe, K., Sequeira, P.C., Agarwalla, S., Rhee, K., Kuhen, K., Phong, W.Y., Patel, V., Beer, D., Walker, J.R., Duraiswamy, J., et al. (2010). A chemical genetic screen in *Mycobacterium tuberculosis* identifies carbon-source-dependent growth inhibitors devoid of in vivo efficacy. Nat. Commun. *1*, 1–8.

Rajashankar, K.R., Bryk, R., Kniewel, R., Buglino, J.A., Nathan, C.F., and Lima, C.D. (2005). Crystal structure and functional analysis of lipoamide dehydrogenase from *Mycobacterium tuberculosis*. J. Biol. Chem. *280*, 33977–33983.

Russell, D.G. (2001). *Mycobacterium tuberculosis*: here today, and here tomorrow. Nat. Rev. Mol. Cell Biol. *2*, 569–577.

Savvi, S., Warner, D.F., Kana, B.D., McKinney, J.D., Mizrahi, V., and Dawes, S.S. (2008). Functional characterization of a vitamin B12-dependent methylmalonyl pathway in *Mycobacterium tuberculosis*: implications for propionate metabolism during growth on fatty acids. J. Bacteriol. *190*, 3886–3895.

Schnappinger, D., Ehrt, S., Voskuil, M.I., Liu, Y., Mangan, J.A., Monahan, I.M., Dolganov, G., Efron, B., Butcher, P.D., Nathan, C., et al. (2003). Transcriptional Adaptation of *Mycobacterium tuberculosis* within Macrophages: Insights into the Phagosomal Environment. J. Exp. Med. *198*, 693–704.

Shi, S., and Ehrt, S. (2006). Dihydrolipoamide acyltransferase is critical for *Mycobacterium tuberculosis* pathogenesis. Infect. Immun. *74*, 56–63.

Singh, V.K., Hattangady, D.S., Giotis, E.S., Singh, A.K., Chamberlain, N.R., Stuart, M.K., and Wilkinson, B.J. (2008). Insertional inactivation of branched-chain alpha-keto acid dehydrogenase in *Staphylococcus aureus* leads to decreased branched-chain membrane fatty acid content and increased susceptibility to certain stresses. Appl. Environ. Microbiol. *74*, 5882–5890.

Smith, H. (2000). Questions about the behaviour of bacterial pathogens in vivo. Philos. Trans. R. Soc. Lond. B Biol. Sci. *355*, 551–564.

St John, G., Brot, N., Ruan, J., Erdjument-Bromage, H., Tempst, P., Weissbach, H., and Nathan, C. (2001). Peptide methionine sulfoxide reductase from *Escherichia coli* and *Mycobacterium tuberculosis* protects bacteria against oxidative damage from reactive nitrogen intermediates. Proc. Natl. Acad. Sci. USA *98*, 9901–9906.

Talaat, A.M., Lyons, R., Howard, S.T., and Johnston, S.A. (2004). The temporal expression profile of *Mycobacterium tuberculosis* infection in mice. Proc. Natl. Acad. Sci. USA *101*, 4602–4607.

Tian, J., Bryk, R., Itoh, M., Suematsu, M., and Nathan, C. (2005a). Variant tricarboxylic acid cycle in *Mycobacterium tuberculosis*: identification of alpha-ketoglutarate decarboxylase. Proc. Natl. Acad. Sci. USA *102*, 10670–10675.

Tian, J., Bryk, R., Shi, S., Erdjument-Bromage, H., Tempst, P., and Nathan, C. (2005b). *Mycobacterium tuberculosis* appears to lack alpha-ketoglutarate dehydrogenase and encodes pyruvate dehydrogenase in widely separated genes. Mol. Microbiol. *57*, 859–868.

Timm, J., Post, F.A., Bekker, L.G., Walther, G.B., Wainwright, H.C., Manganelli, R., Chan, W.T., Tsenova, L., Gold, B., Smith, I., et al. (2003). Differential expression of iron-, carbon-, and oxygen-responsive mycobacterial genes in the lungs of chronically infected mice and tuberculosis patients. Proc. Natl. Acad. Sci. USA *100*, 14321–14326.

Toal, D.R., Clifton, S.W., Roe, B.A., and Downard, J. (1995). The *esg* locus of *Myxococcus xanthus* encodes the E1 alpha and E1 beta subunits of a branched-chain keto acid dehydrogenase. Mol. Microbiol. *16*, 177–189.

Upton, A.M., and McKinney, J.D. (2007). Role of the methylcitrate cycle in propionate metabolism and detoxification in *Mycobacterium smegmatis*. Microbiology *153*, 3973–3982.

Zhang, S.Y., Boisson-Dupuis, S., Chapgier, A., Yang, K., Bustamante, J., Puel, A., Picard, C., Abel, L., Jouanguy, E., and Casanova, J.L. (2008). Inborn errors of interferon (IFN)-mediated immunity in humans: insights into the respective roles of IFN-alpha/beta, IFN-gamma, and IFN-lambda in host defense. Immunol. Rev. *226*, 29–40.